VALIDATED STUDY OF THE EXISTENCE OF SHORT CYCLES FOR CHAOTIC SYSTEMS USING SYMBOLIC DYNAMICS AND INTERVAL TOOLS

ZBIGNIEW GALIAS
Department of Electrical Engineering, AGH University of Science and Technology,
Mickiewicza 30, 30–059 Kraków, Poland
galias@agh.edu.pl

WARWICK TUCKER
Department of Mathematics, Uppsala University,
Box 480, 751 06 Uppsala, Sweden
warwick@math.uu.se

Received (to be inserted by publisher)

We show that, for a certain class of systems, the problem of establishing the existence of periodic orbits can be successfully studied by means of a symbolic dynamics approach combined with interval methods. Symbolic dynamics is used to find approximate positions of periodic points, and the existence of periodic orbits in a neighborhood of these approximations is proved using an interval operator. As an example the Lorenz system is studied; a theoretical argument is used to prove that each periodic orbit has a distinct symbol sequence. All periodic orbits with the period $p \leq 16$ of the Poincaré map associated with the Lorenz system are found. Estimates of the topological entropy of the Poincaré map and the flow, based on the number and flow-times of short periodic orbits, are calculated. Finally, we establish the existence of several long periodic orbits with specific symbol sequences.

Keywords: periodic orbit, symbolic dynamics, interval arithmetic, Lorenz system

1. Introduction

Understanding and describing the long–term dynamics of a chaotic attractor, stemming from a continuous-time differential system is a very challenging task. Many advances in this direction have been made concerning *qualitative* properties, often resulting in statistical/probabilistic statements, [Benedicks & Carleson, 1991; Luzzatto *et al.*, 2005]. When it comes to *quantitative* assertions, however, very little progress has been made. The main reason for this is that classical mathematics lacks the tools to extract the relevant pieces of information from global continuous differential systems. Even finding periodic orbits of the system remains challenging. A grand example of the difficulties one faces is illustrated by Hilbert's 16th problem, where the number of limit cycles a planar, polynomial differential system can have is sought. After more than a century, this question remains unanswered even in the quadratic case.

A chaotic attractor is densely filled by its (unstable) periodic orbits. Thus, an increasingly good picture of the dynamics is obtained by considering increasingly long periodic orbits. Unstable periodic orbits can be stabilized by the use of feedback, converting a chaotic system into a controllable one [Ott *et al.*, 1990]. These techniques have been applied to e.g. lasers [Bielawski *et al.*, 1994] and diode resonators [Gauthier

et al., 1994]. For an introduction to the field of continuous dynamical systems, see e.g. [Strogatz, 2001].

With the advent of computer-aided proofs, based on set–valued computations [Moore, 1966; Neumaier, 1990], several methods for finding periodic orbits have been introduced. An important class of such methods use interval operators [Krawczyk, 1969; Neumaier, 1990] applied to a Poincaré map associated with the continuous system under consideration. When these methods are combined with approximations of periodic orbits, they can be used to locate many cycles embedded in chaotic attractors.

Finding all short periodic orbits of dynamical systems is even more challenging. It is known that this problem can be solved successfully for some discrete systems [Galias, 2001, 2002] and for a certain class of continuous systems including the Rössler system [Galias, 2006]. The technique is based on the construction of the graph describing the dynamics of the system, and finding in the graph all short cycles corresponding to periodic solutions. This general technique, however, is not directly applicable to the class of systems whose attractors (like the Lorenz attractor) contain an unstable equilibrium. For such systems there exist trajectories for which the return time is arbitrarily long. Standard techniques for rigorous integration of a continuous system near such trajectories are unusable; the evaluation procedure often fails or produces unusable results due to huge overestimation. This makes the graph based technique unsuitable for finding all short periodic orbits even of relatively small lengths.

The Lorenz system [Lorenz, 1963] is well understood in terms of geometric models [Sparrow, 1982]. Many researchers studied this system using rigorous computer assisted methods. The Lorenz system has been shown to be chaotic in the topological sense for the case of non-classical [Mischaikow & Mrozek, 1995] and classical [Galias & Zgliczyński, 1998] parameter values. The existence of a strange attractor for this system has been proved in [Tucker, 1999].

In this work, we address the problem of proving the existence of short periodic orbits in the Lorenz system. We use special properties of the Lorenz attractor which, combined with interval tools, allow us to find all periodic orbits of relatively large length.

The paper is organized as follows. In Sec. 2 we describe two methods to find all short cycles. The first one is a general technique based on the construction of a graph describing the dynamics of the system, while the second one uses the symbolic dynamics approach. The second method is applicable to systems for which there exists symbolic dynamics uniquely characterizing periodic solutions. This symbolic dynamics based approach is used to find approximate positions of periodic points. When combined with interval tools for testing the existence of periodic orbits this method makes it possible to find all short cycles with much longer periods than the first technique.

The results on applications of both methods for finding short periodic orbits for the Lorenz system are presented in Sec. 3. Estimates of topological entropy of the Poincaré map and the flow based on the number and flow-times of short periodic orbits are calculated. In the last section the method is applied to prove the existence of several long periodic orbits with specific symbol sequences.

Following the convention in the literature on interval arithmetic, we will denote interval objects: intervals, interval vectors and interval matrices by bold letters.

2. Finding all short periodic orbits

First, let us briefly recall a general method which can be used to find all short periodic orbits for a continuous dynamical system [Galias, 2006]. The first step is a reduction of the continuous-time system to a discrete system using the concept of a Poincaré map.

2.1. *Poincaré map*

The *Poincaré map* (also called the *return map*) $R : \Sigma \mapsto \Sigma$ is defined as $R(x) = \varphi(\tau(x), x)$, where $\Sigma = \Sigma_1 \cup \cdots \cup \Sigma_m$ is the union of hyperplanes and $\tau(x)$ is the return time after which the trajectory $\varphi(t, x)$ returns to Σ. Periodic points of R correspond to periodic orbits of the continuous system.

In order to study the existence of period–p orbits of R we construct the map F defined by

$$[F(z)]_k = x^{((k+1) \bmod p)} - R(x^{(k)}) \text{ for } 0 \le k < p, \tag{1}$$

where $z = (x^{(0)}, x^{(1)}, \ldots, x^{(p-1)})$. Zeros of F correspond to period–p points of R, i.e. $F(z)=0$ if and only if $R^p(x^{(0)}) = x^{(0)}$.

2.2. *Interval methods*

Interval methods provide simple computational tests for uniqueness, existence, and nonexistence of zeros of a map within a given interval vector. In order to investigate the existence of zeros of F in the interval vector $\mathbf{z}$ one evaluates an interval operator over $\mathbf{z}$. In this work we use the Krawczyk operator [Krawczyk, 1969; Neumaier, 1990]:

$$\mathrm{K}(\mathbf{z}) = \hat{z} - CF(\hat{z}) - (CF'(\mathbf{z}) - I)(\mathbf{z} - \hat{z}), \tag{2}$$

where $\hat{z} \in \mathbf{z}$, $F'(\mathbf{z})$ is the interval matrix containing the Jacobian matrices $F'(z)$ for all $z \in \mathbf{z}$, and C is an invertible matrix. In our implementation, we choose $\hat{z}$ to be the center of $\mathbf{z}$, and the preconditioning matrix C to be the inverse of $F'(\hat{z})$.

There are other possible choices, like the interval Newton operator or the Hansen–Sengupta operator, but in this case they are outperformed by the Krawczyk method.

The most important property of the Krawczyk operator can be used to prove the existence and uniqueness of zeros. It states that if $\mathrm{K}(\mathbf{z}) \subset \operatorname{int}\mathbf{z}$, where $\operatorname{int}\mathbf{z}$ denotes the interior of $\mathbf{z}$, then F has exactly one zero in $\mathbf{z}$. The second property provides the non-existence test: if $\mathrm{K}(\mathbf{z}) \cap \mathbf{z} = \emptyset$, then there are no zeros of F in $\mathbf{z}$. Note that all operations in (2), including evaluation of $F(\hat{z})$ and $F'(\mathbf{z})$, have to be implemented rigorously in interval arithmetic for these properties to be valid.

In order to evaluate the interval operator for the map F defined by (1) over the interval vector $\mathbf{z} = (\mathbf{x}^{(0)}, \mathbf{x}^{(1)}, \ldots, \mathbf{x}^{(p-1)})$, we need a method to find an enclosure of $R(\mathbf{x}^{(k)})$ and an enclosure of the Jacobian $R'(\mathbf{x}^{(k)})$ for $0 \le k < p$. These enclosures are found in interval arithmetic by rigorous integration of the differential equation and its variational equation. For details see [Galias, 2006].

2.3. *Finding all short cycles*

In this section, we describe briefly how to use a combination of interval tools and generalized bisection to find all short periodic orbits enclosed in a certain region. First, the region of interest is covered by boxes (interval vectors) and the dynamics of R is represented in a form of the directed graph. In the graph representation, boxes are graph vertices, and non-forbidden transitions between boxes are graph edges. This representation is found rigorously by computing for each box $\mathbf{v}_i$ an enclosure $\mathbf{w}_i$ of its image $R(\mathbf{v}_i)$, and finding all boxes which have nonempty intersection with $\mathbf{w}_i$. Next, for each period–p cycle in the graph, the interval operator K is evaluated over the interval vector $\mathbf{z}$ corresponding to this cycle. If $\mathbf{z} \cap \mathrm{K}(\mathbf{z}) = \emptyset$, then there are no period–p orbits in $\mathbf{z}$. If $\mathrm{K}(\mathbf{z}) \subset \operatorname{int}\mathbf{z}$, then there exists exactly one period–p orbit in $\mathbf{z}$ (p is not necessarily the principal period of the orbit). If neither of the above two conditions is satisfied the search procedure fails, and we may try to repeat the computation using smaller boxes.

Usually many cycles in the graph correspond to a single periodic orbit and therefore this approach may fail due to the long computation time needed to check all cycles. To reduce the number of cycles to be considered one may for example generate the graph representation for a finer covering and then locate cycles for a coarser covering. For details see Sec. 3.

2.4. *Symbolic dynamics approach*

For a certain class of systems it is possible to construct symbolic dynamics which uniquely characterizes periodic orbits. Let us assume that the state space is divided into disjoint sets $N_1, N_2 \ldots, N_m$. We associate a *symbol sequence* $(s_k)_{k=0}^{\infty}$, where $s_k \in \{1, 2, \ldots, m\}$ with a trajectory $(x_k)_{k=0}^{\infty}$, in such a way that $x_k \in N_{s_k}$. In the following, we assume that each periodic orbit corresponds to a unique periodic symbol sequence. This assumption is essential if we want to locate all short periodic orbits in a rigorous way.

Now, we describe how to prove the existence of the periodic orbit with the given symbol sequence $s = (s_0, s_1, \ldots, s_{p-1})$. Let us assume that we have a long computer generated trajectory $(x^{(0)}, x^{(1)}, \ldots, x^{(N-1)})$ with the associated symbol sequence $(r_0, r_1, \ldots, r_{N-1})$. First, in order to guess an approximate position of

the periodic orbit, we find for each $0 \le k < p-1$ a position j_k in the data set $(x^{(i)})$ for which the future symbol sequence $(r_{j_k}, r_{j_k+1}, r_{j_k+2}, \ldots)$ matches the sequence $(s_k, s_{k+1}, s_{k+2}, \ldots)$ as long as possible, where for $i \ge p$ we define $s_i = s_{i \bmod p}$. The vector $z = (x^{(j_0)}, x^{(j_1)}, \ldots, x^{(j_{p-1})})$ serves as an initial guess for the position of the periodic orbit with the symbol sequence s. Next, we use the standard (non-interval) Newton iteration to find a better approximation of the position of the periodic orbit in a neighborhood of z, and finally we prove the existence of a nearby true periodic orbit using the Krawczyk operator.

To locate all periodic orbits of period p it is sufficient to carry out the procedure described above for all periodic symbol sequences with the principal period p. From the assumption that each periodic orbit has a unique symbol sequence it follows immediately that one does not have to consider periodic orbits with the principal period smaller than p. From the uniqueness property they have to correspond to a shorter periodic orbit.

It may happen that there is no periodic orbit with a certain symbol sequence s. In such a case we have to use the graph based method to exclude the existence of an orbit with the symbol sequence s. Let us note however that for large p only very few cycles in the graph correspond to a single symbol sequence, when compared to the total number of period–p cycles in the graph. Therefore, using symbolic dynamics information can also be useful for non-existence tests.

3. Periodic orbits for the Lorenz system

In this section, we study the existence of periodic orbits for the Lorenz system. The Lorenz system is described by the following set of equations

$$\begin{aligned} \dot{x}_1 &= s x_2 - s x_1, \\ \dot{x}_2 &= r x_1 - x_2 - x_1 x_3, \\ \dot{x}_3 &= x_1 x_2 - q x_3. \end{aligned} \tag{3}$$

We consider the Lorenz system with the classical parameter values: $s = 10$, $r = 28$, $q = 8/3$. An example trajectory of the Lorenz system is shown in Fig. 1.

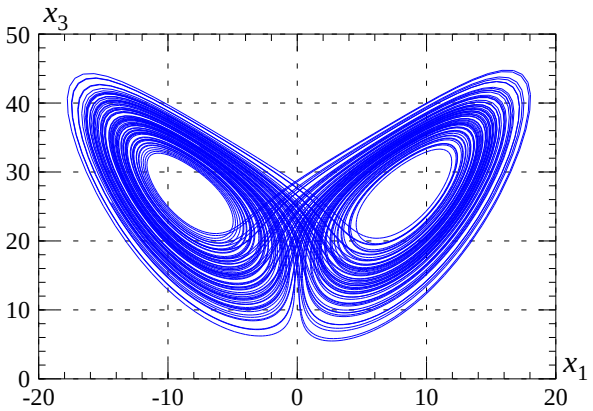

Fig. 1. A trajectory of the Lorenz system

For these parameter values, the Lorenz system has three equilibria. One of them is the origin. It has one positive eigenvalue $\lambda_1 \approx 11.8277$ and two negative eigenvalues $\lambda_2 \approx -22.8277$ and $\lambda_3 \approx -2.6667$. The other two equilibria have a pair of complex eigenvalues with positive real parts $\mu_{1,2} \approx 0.094 \pm i10.19$, and one real negative eigenvalue $\mu_3 \approx -13.854$.

For some computations (especially those involving trajectories passing close to the origin) it is convenient to use the diagonal form of the Lorenz system, where the invariant manifolds of the origin are tangent

to the coordinate axes:

$$\begin{aligned}\dot{x}_1 &= \lambda_1 x_1 - k_1(x_1 + x_2)x_3,\\ \dot{x}_2 &= \lambda_2 x_2 + k_1(x_1 + x_2)x_3,\\ \dot{x}_3 &= \lambda_3 x_3 + (x_1 + x_2)(k_2 x_1 + k_3 x_2).\end{aligned} \tag{4}$$

The diagonal form is obtained using a linear change of variables. The constants are given by $k_1 = s/u$, $k_{2,3} = (s-1\pm u)/(2s)$, $\lambda_{1,2} = (-s-1\pm u)/2$, $\lambda_3 = -q$, where $u = \sqrt{(s+1)^2 + 4s(r-1)}$.

Since the change of variables is linear, it has no influence on the number or stability properties (Floquet multipliers) of periodic orbits. Nor does it affect the symbolic dynamics.

3.1. *Trapping region and average return time*

Let us choose the Poincaré map R defined by the hyperplane $\Sigma = \{x = (x_1, x_2, x_3)\colon x_3 = 27, \dot{x}_3 < 0\}$ and the system (4).

We begin our analysis of the existence of periodic orbits in the Lorenz attractor by finding a trapping region containing the attractor of R. Observe that this cannot be done by a direct integration of the differential equation seeing that there are trajectories in the Lorenz attractor which pass arbitrarily close to the origin, and for which the return time is arbitrarily long. The trapping region is found using a modified Euler method with rigorous error bounds. In order to reduce expansion along the trajectories we use partitioning. When a box has expanded enough, it is partitioned, and the sub–boxes are then treated separately. This helps to reduce problems associated with the wrapping effect. Trajectories passing close to the fixed point at the origin are treated differently. We define a cube around the origin, and interrupt computations if the trajectory hits the cube. We then change to the normal form coordinates and explicitly compute the exit of the trajectory. There are two different ways in which a box can pass through the cube. If the box intersects the stable manifold of the origin, it is split along the line of intersection, and exits the cube in two pieces. Otherwise, the box flows out in one piece. After leaving the cube, we switch back to the original coordinates, and resume numeric computations. For details see [Tucker, 1999].

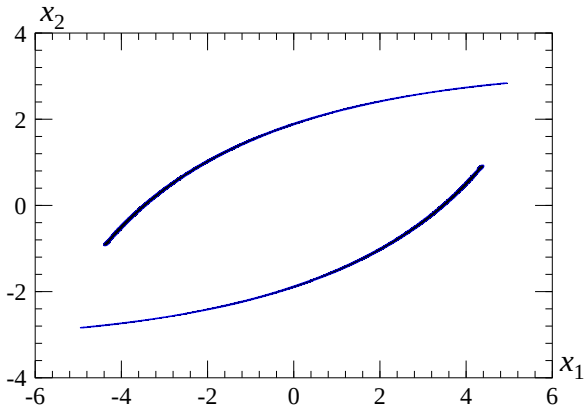

Fig. 2. Trapping region for the Poincaré map R

The trapping region is composed of 14518 boxes of size $1/2^7 \times 1/2^7$ (see Fig. 2). There are 514126 connections in the corresponding graph.

Using information on return times for individual boxes, we can find bounds for the return time of the kth iterate of R. Since for some boxes an upper bound for the return time is infinite, the return time for the whole attractor is unbounded. Lower bounds t_k of return times for R^k are collected in Table 1.

It is clear that the average return time τ_{aver} between two crossings is larger than t_k/k for each k. For $k = 10000$ we obtain:

$$\tau_{\text{aver}} > 0.6397. \tag{5}$$

Table 1. Lower bound t_k of return times for R^k

k	t_k	t_k/k
1	0.537044	0.537044
2	1.147434	0.573717
5	2.981325	0.596265
10	6.047894	0.6047894
100	63.721019	0.63721019
1000	639.204730	0.63920473
10000	6397.362682	0.6397362682

It follows that the flow-time of any periodic orbit corresponding to a period–p cycle of R is larger than $p \cdot 0.6397$.

3.2. *Periodic orbits by the graph-based approach*

In this section, we present results on the existence of periodic orbits of R obtained using the graph-based approach. There are no period–1 cycles in the graph, hence there are no period–1 orbits.

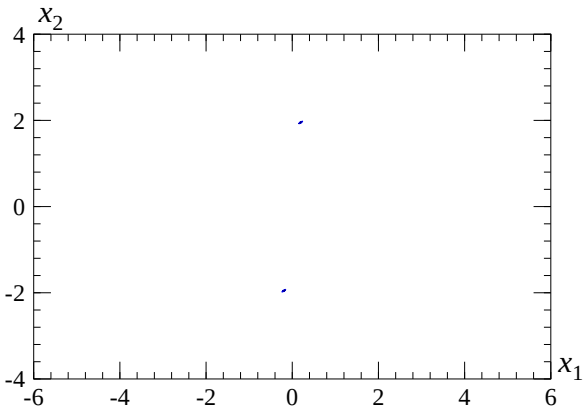

Fig. 3. Regions containing all periodic orbits of the map R with the period $p = 2, 3, 4$, $x_3 = 27$

In order to study the existence of period–2 orbits, a set of boxes containing all period–2 cycles is found. This set is composed of 86 boxes, which form two connected components (see Fig. 3(a)).

The application of the method for finding all period–2 orbits is unsuccessful for this set due to long return times and strong stretching. One way to overcome this difficulty is to introduce additional sections for the Poincaré map to shorten return times. Let us now consider the Poincaré map R_1 defined by the set $\Sigma = \Sigma_1 \cup \Sigma_2$, where $\Sigma_1 = \{x\colon x_3 = 27\}$, $\Sigma_2 = \{x\colon x_3 = 14\}$. The planes $\Sigma_{1,2}$ are selected in such a way that period–2 orbits of the original map R correspond to period–8 orbits of the map R_1. We start by generating the graph for R_1. The graph has 182 boxes and 638 connections. There are 26086 period–8 cycles in the graph.

In order to reduce the number of cycles, we regenerate the graph at a higher accuracy, and then come back to the original box size. This procedure significantly reduces the number of cycles to be considered. Dividing each box into 16×16 smaller boxes, and generating the graph for this division we arrive at a covering composed of 216 boxes of size $1/2^{11} \times 1/2^{11}$ with 724 connections. Coming back to the original box size gives 16 boxes and 24 connections.

At this stage we can apply the techniques described in Section 2 to find all period–8 orbits of R_1. There are 36 cycles of length 8 in the graph. The Krawczyk operator is evaluated for each cycle, and it is verified that only one of them corresponds to a periodic orbit. This periodic orbit is self-symmetric

(compare Fig. 7(a)).

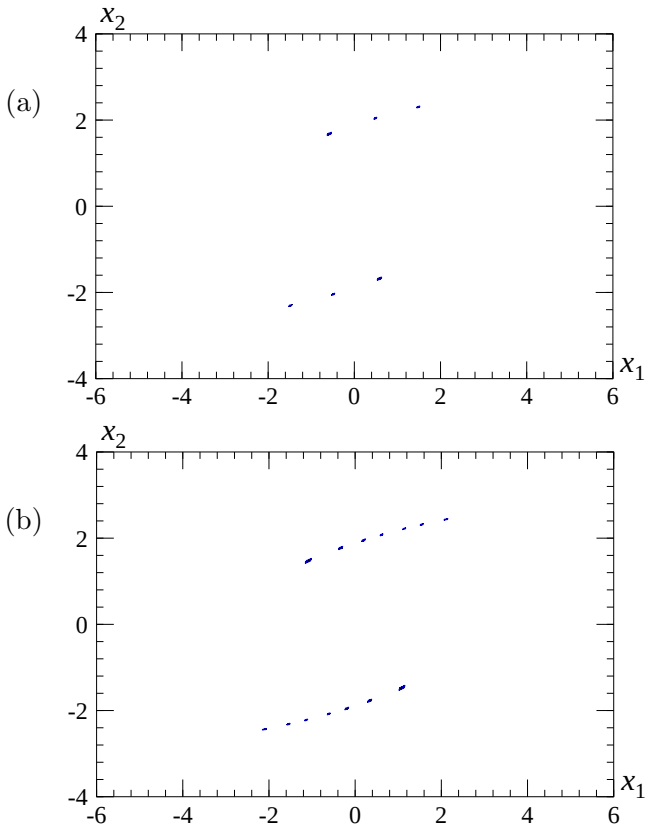

Fig. 4. Regions containing all periodic orbits of the map R with the period $p = 2, 3, 4$, $x_3 = 27$

Similar computations have been performed for periods $p \in \{3, 4\}$. The set containing all period-3 cycles is composed of 254 boxes (see Fig. 3(a)). Introducing sections $\Sigma_1 = \{x\colon x_3 = 27\}$, $\Sigma_2 = \{x\colon x_3 = 18\}$ we obtain a graph composed of 636 cycles and 2748 connections. To reduce the number of cycles, we consider boxes of size $1/2^{13} \times 1/2^{13}$. The resulting graph has 460 boxes and 1500 connections. Increasing the box size, we obtain a set of 38 boxes of size $1/2^9 \times 1/2^9$ with 54 connections. There are 72 period–12 cycles in the graph. Two of them correspond to periodic orbits. They are symmetric to each other. One of them is plotted in Fig. 7(b).

For the case $p = 4$ there are 654 boxes covering period–4 orbits of R (see Fig. 3(b)). Using sections $\Sigma_1 = \{x\colon x_3 = 27\}$, $\Sigma_2 = \{x\colon x_3 = 19\}$ we obtain a graph composed of 2220 boxes with 15516 connections. Considering the box size $1/2^{17} \times 1/2^{17}$, we obtain 3166 boxes with 21450 connections. Increasing the box size, we obtain a set of 72 boxes of size $1/2^{10} \times 1/2^{10}$ with 90 connections. Out of 188 period–16 cycles three correspond to periodic orbits. There is a pair of orbits symmetric to each other and one self-symmetric orbit (see Fig. 7(c,d)).

Summarizing, we have proved the existence of exactly six periodic orbits with period $p \leq 4$. For longer periods ($p \geq 5$) the graph based method fails due to long computation time, and the necessity of introducing many intermediate sections for the Poincaré map. In the next section, we present results obtained using a much more effective symbolic dynamics based approach.

3.3. *Periodic orbits by the symbolic dynamics based approach*

In [Tucker, 1999, 2002], it was shown that the Poincaré map induces a stable foliation of the forward invariant part of Σ. It follows that a periodic symbol sequence corresponds to at most one periodic orbit. This fact is now explained in more detail.

Let $S\colon \mathbb{R}^3 \to \mathbb{R}^3$ be defined by $(x_1, x_2, x_3) \mapsto (x_1, -x_2, -x_3)$. In [Tucker, 2002] it was established that there exists a finite set of rectangles $N = N^- \cup N^+ \subset \Sigma$ where $N^- = \cup_{k=1}^{M} N_k^-$ and $N^+ = S(N^-)$ such that N is mapped into itself by the return map $R\colon \Sigma \to \Sigma$ induced by the flow of the Lorenz equations (4). Thus N is a *trapping region* for the return map: $R(N) \subset N$, and we can form the forward invariant set $\mathcal{A} = \cap_{k=0}^{\infty} P^k(N)$. In fact, $\mathcal{A}$ is the intersection of the Lorenz attractor with N, see [Tucker, 2002].

Given a trajectory starting in N, we can code it in terms of two symbols, indicating which of the two (disjoint) branches N^- or N^+ is currently being visited. In other words, for a trajectory $\{x_n\}_{n=0}^{\infty} \subset N$, where $x_{n+1} = R(x_n)$ we form the associated symbol sequence $s = (s_0, s_1 \dots)$ defined by $s_n = -1$ if $x_n \in N^-$ and $s_n = +1$ if $x_n \in N^+$.

In order to study periodic orbits we consider periodic symbol sequences $s = (s_0, s_1, \dots, s_{p-1})$, where $s_k \in \{-1, +1\}$, for $0 \le k < p$. Non-rigorous computations indicate that each periodic symbol sequence with no more than 24 repeating symbols corresponds to a periodic orbit (compare [Viswanath, 2003]). The following theorem allows us to use the symbolic dynamics approach to find all short periodic cycles for the Lorenz system.

Theorem 1. *Let $N \subset \Sigma$ be the trapping region mentioned above. Given a periodic symbol sequence $s = (s_0, s_1, \dots, s_{p-1})$, there exists* at most *one point $x \in N$ with the symbol sequence s such that $R^p(x) = x$.*

Proof. First, we note that any periodic orbit in the trapping region N also belongs to the attractor $\mathcal{A}$ itself. Second, by the hyperbolicity estimates from [Tucker, 2002], we know that N is foliated by "vertical" stable leaves. A dense set of these leaves is made up of the intersections of the stable manifold of the origin with the trapping region $W^s(0) \cap N$. The stable manifold of the origin is defined as $W^s(0) = \{x \in \mathbb{R}^3 \colon \lim_{t\to\infty} \varphi(t, x) = 0\}$.

Now suppose, by contradiction, that R^p has two distinct fixed points, $x, y \in N$, having the same symbol sequence $s = (s_0, s_1, \dots, s_{p-1})$. Then we face one of two possible scenarios.

(1) The points x and y belong to the same stable leaf of the foliation of the trapping region N. If this is the case, then the distance $\|R^{kp}(x) - R^{kp}(y)\|$ tends to zero as k goes to infinity. It follows that $x = y$ seeing that both x and y have period p.

(2) The points x and y belong to distinct stable leaves of the foliation of the trapping region N. Let Γ be the leaf in $W^s(0) \cap N$ that contains the point $(0, 0, 27)$. This is the first intersection between $W^s(0)$ and N. In this case we can find a stable leaf $\gamma \subset R^{-k}(\Gamma) \cap N$ that "vertically" separates x and y. This leads to a contradiction as $R^{k+1}(x)$ and $R^{k+1}(y)$ will have different symbols. ■

We have applied the method presented in Section 2 to find all short periodic orbits for the map R. From now on we switch back to the original Lorenz system. Consequently, the map R is the return map defined by the hyperplane $\Sigma = \{x = (x_1, x_2, x_3) \colon x_3 = 27, \dot{x}_3 < 0\}$ and the system (3).

In the first step, a trajectory of R is generated (see Fig. 5).

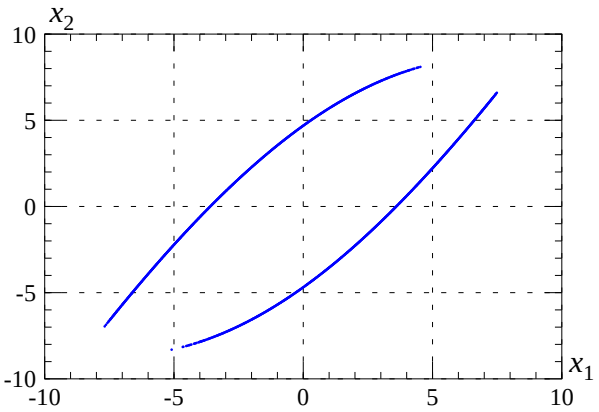

Fig. 5. A computer generated trajectory of R with 10^6 points

The trajectory should be long and should cover the attractor as densely as possible. If this is the case then all short admissible symbol sequences can be found in this trajectory. In Table 2 the numbers of symbol sequences of various length realized by a generated trajectory are reported. The total number $l_p = 2^p$ of all symbol sequences of length p is given for comparison. Two examples of trajectories of lengths 10^5 and 10^6 are considered. In both cases all symbol sequences up to length 12 are present. Note that for the shorter data set only 16% (9%) of symbol sequences of length 19 (20) are present. For the longer data set all symbol sequences up to length 15 are present and 76% (54%) of symbol sequences of length 19 (20) are present. It is clear that the longer data set provides much better approximations of positions of points with a given sequence of symbols.

Table 2. The numbers l'_p and l''_p of symbol sequences of length p present in data files containing 10^5 and 10^6 points, $l'_p = l''_p = l_p = 2^p$ for $p \leq 12$

p	l'_p	l''_p	$l_p = 2^p$
12	4096	4096	4096
13	8185	8192	8192
14	16051	16384	16384
15	29061	32768	32768
16	45880	65521	65536
17	62713	129931	131072
18	76315	242853	262144
19	85920	400018	524288
20	92002	569806	1048576

In the second step, we consider all periodic symbol sequences with the principal period $p \leq 16$. Clearly, it is sufficient to choose one of the symbol sequences corresponding to each cycle; it does not make sense to check both sequences $(s_1, s_2, \ldots, s_p)$ and $(s_2, s_3, \ldots, s_p, s_1)$ since they correspond to the same periodic orbit. One can also skip symbol sequences for which the principal period is smaller than p; as explained before they correspond to shorter periodic orbits. The number of symbol sequences can be further reduced using the symmetry of the Lorenz system; if the symbol sequence $(s_1, s_2, \ldots, s_p)$ corresponds the the orbit with the initial condition (x_1, x_2, x_3) then the symbol sequence $(-s_1, -s_2, \ldots, -s_p)$ corresponds the the orbit with the initial condition $(x_1, -x_2, -x_3)$.

From the graph based approach we know that both symbol sequences with the principal period $p = 1$, i.e. $s = (-1)$ and $s = (+1)$ are not admissible. From the Theorem 1 we know that every other sequence corresponds to *at most* one periodic orbit of R. We have verified that indeed for each symbol sequence with the principal period $2 \leq p \leq 16$ there exist a periodic orbit with this symbol sequence. There are 38 self symmetric orbits. These are periodic orbits with symmetric symbol sequences, for example: $(-+)$, $(--++)$, $(---+++)$, $(----++++)$, $(--+--++-+)$. There are also 4380 pairs of orbits symmetric to each other. This gives the total number of 8798 periodic orbits with period $p \leq 16$. Let us note that there are exactly 8798 periodic symbol sequences with period $p \in \{2, 3, \ldots, 16\}$ and recall that each periodic symbol sequence corresponds to at most one periodic orbit. Hence, we have confirmed that there are exactly 8798 periodic orbits of R with the period $p \leq 16$ (compare [Viswanath, 2003]).

The results concerning periodic orbits of specific periods are collected in Table 3. For each $p \leq 16$ the number q_p of period–p orbits of R is given. We also report the number $q_p^{(\mathrm{s})}$ of self-symmetric period–p cycles, the number $q_p^{(\mathrm{ns})}$ of pairs of non-symmetric period–p cycles, and bounds $\mathbf{T}_p$ for flow-times. It is interesting to note that some of the period–11 orbits are longer than shortest period–12 orbits. A similar phenomenon is observed for longer periods. The average return time for periodic orbits with principal period p is also reported. Let us notice that the shortest periodic orbit (the one with the symbol sequence $(-+)$) has the longest average flow-time. Out of the period–p orbits the shortest average flow-time is attained by orbits with the sequence composed of $p-1$ equal symbols followed by one opposite symbol. This is somewhat unexpected, since those orbits come close to the origin, and trajectories passing there have long return

times. Apparently, this long return time is fully compensated by the short return times of other points along these orbits. On the other hand, the longest average flow-time is achieved by the orbit with the sequence composed of alternating $-$ and $+$ symbols followed by $-$ for p odd, and by $(+-)$ for p even. For increasing p, these orbits become more and more similar in terms of the symbol sequence to the shortest periodic orbit with the sequence $(-+)$, and therefore it is expected that their average return time converges to the average return time of the shortest orbit. Observe also that the greatest average return times for odd (even) p grow monotonically with p and that for even $p \geq 6$ they are smaller than for odd $p-1$.

Table 3. Short periodic orbits of R, the number q_p of period–p cycles, the number $q_p^{(\mathrm{ns})}$ of pairs of non-symmetric period–p cycles, the number $q_p^{(\mathrm{s})}$ of self-symmetric period–p cycles, rigorous bounds $\mathbf{T}_p$ for flow-times of period–p cycles, rigorous bounds $\mathbf{T}_p/p$ for average flow-times of period–p cycles, $\underline{s}_p$ and $\overline{s}_p$ are period–p sequences corresponding to orbits with the shortest and longest average flow-times

p	q_p	$q_p^{(\mathrm{ns})}$	$q_p^{(\mathrm{s})}$	$\mathbf{T}_p$	$\mathbf{T}_p/p$	$\underline{s}_p$	$\overline{s}_p$
1	0	0	0	—	—		
2	1	0	1	1.558652^{40}_{05}	0.779326^{200}_{025}	$-+$	$-+$
3	2	1	0	2.305907^{55}_{00}	0.768635^{85}_{66}	$--+$	$--+$
4	3	1	1	$[3.02358, 3.08428]$	$[0.75589, 0.77107]$	$---+$	$--++$
5	6	3	0	$[3.72564, 3.86954]$	$[0.74512, 0.77391]$	$(-)^4+$	$-(-+)^2$
6	9	4	1	$[4.41776, 4.63715]$	$[0.73629, 0.77286]$	$(-)^5+$	$-(-+)^2+$
7	18	9	0	$[5.10303, 5.42913]$	$[0.72900, 0.77559]$	$(-)^6+$	$-(-+)^3$
8	30	14	2	$[5.78340, 6.19461]$	$[0.72292, 0.77433]$	$(-)^7+$	$-(-+)^3+$
9	56	28	0	$[6.46025, 6.98798]$	$[0.71780, 0.77645]$	$(-)^8+$	$-(-+)^4$
10	99	48	3	$[7.13463, 7.75301]$	$[0.71346, 0.77531]$	$(-)^9+$	$-(-+)^4+$
11	186	93	0	$[7.80735, 8.54668]$	$[0.70975, 0.77698]$	$(-)^{10}+$	$-(-+)^5$
12	335	165	5	$[8.47920, 9.31162]$	$[0.70660, 0.77597]$	$(-)^{11}+$	$-(-+)^5+$
13	630	315	0	$[9.15092, 10.10534]$	$[0.70391, 0.77734]$	$(-)^{12}+$	$-(-+)^6$
14	1161	576	9	$[9.82315, 10.87025]$	$[0.70165, 0.77645]$	$(-)^{13}+$	$-(-+)^6+$
15	2182	1091	0	$[10.49656, 11, 66399]$	$[0.69977, 0, 77760]$	$(-)^{14}+$	$-(-+)^7$
16	4080	2032	16	$[11.17200, 12.42890]$	$[0.69825, 0, 77681]$	$(-)^{15}+$	$-(-+)^7+$
1–16	8798	4380	38	$[1.55865, 12.42890]$	$[0.69825, 0.77933]$	$(-)^{15}+$	$-+$

The positions of periodic orbits with the period $p \leq 16$ are plotted in Fig. 6. One can see that they tend to fill the middle part of the attractor, and that the area occupied by period–p orbits grows with p. Also note that even for the largest p considered, there are visible gaps in the plots, meaning that there are no short cycles in these areas.

The flow-time of any other periodic orbit of R is larger than $17 \cdot 0.6397 = 10.8749$ (compare Eq. (5)). Since the shortest 2552 periodic orbits found (including all periodic orbits with period $p \leq 14$) have flow-times shorter than 10.8749, it follows that these periodic orbits are indeed the shortest. Note that from the bound (5) we cannot conclude that all cycles with the period $p > 16$ have flow-times longer than all period–15 orbits.

The results concerning periodic orbits with period $p \leq 8$ are collected in Table 4. For each orbit its period p, the interval $\mathbf{T}$ containing the flow-time, and the corresponding symbol sequence are reported. Periodic orbits with period $p \leq 6$ are plotted in Fig. 7. For each pair of symmetric orbits only one is plotted.

3.4. *Estimates for topological entropy*

Using the number of short cycles one can obtain estimates for the topological entropy of the map. Under certain assumptions (see [Bowen, 1971]) the topological entropy $\mathrm{h}(f)$ of a map f is related to the number of periodic orbits by $\mathrm{h}(f) = \limsup_{p\to\infty} p^{-1} \log \mathrm{P}_p$ where P_p denotes the number of fixed points of f^p.

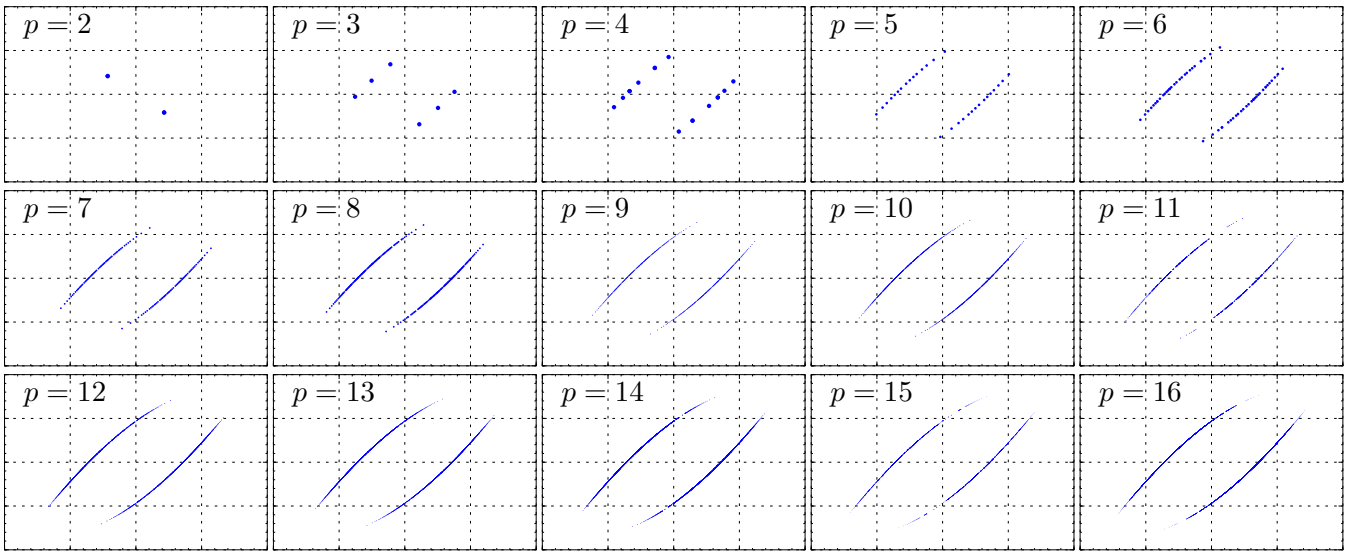

Fig. 6. All periodic orbits of R with the period $n \leq 16$

Table 4. Short periodic orbits of R, p — the period of the orbit, '*' denotes a self-symmetric orbit, **T** — bounds for the flow-time, s — the corresponding symbol sequence

p	**T**	s	p	**T**	s	p	**T**	s
*2	1.558652^{40}_{05}	$-+$	7	5.23419^{90}_{74}	$------++$	8	6.03523^{34}_{16}	$-----+-+$
3	2.305907^{55}_{00}	$--+$	7	5.28634^{22}_{07}	$-----+++$	8	6.08235^{89}_{71}	$-----+-++$
4	3.02358^{41}_{33}	$---+$	7	5.301^{2013}_{1998}	$-----+-+$	8	6.08382^{78}_{61}	$-----++-+$
*4	3.08427^{71}_{64}	$--++$	7	5.33091^{31}_{16}	$----+--+$	8	6.10805^{54}_{38}	$----+-+++$
5	3.72564^{24}_{12}	$-----+$	7	5.3698^{812}_{797}	$----+-++$	8	6.12145^{55}_{39}	$----+--++$
5	3.82025^{47}_{37}	$----++$	7	5.37052^{63}_{50}	$----++-+$	8	6.12233^{73}_{56}	$----++--+$
5	3.86953^{97}_{86}	$--+-+$	7	5.3942^{176}_{61}	$--+---++$	8	6.1351^{279}_{62}	$----++-++$
6	4.41776^{72}_{58}	$------+$	7	5.4291^{261}_{246}	$--+-+-+$	8	6.1547^{203}_{186}	$----+-+-+$
6	4.53410^{85}_{73}	$-----++$	8	5.7834^{121}_{097}	$-------+$	8	6.1758^{796}_{780}	$--+--+-+$
*6	4.56631^{18}_{05}	$----+++$	8	5.9249^{949}_{930}	$-------++$	*8	6.1875^{199}_{183}	$--+-++-+$
6	4.59381^{50}_{38}	$----+-+$	8	5.9904^{445}_{428}	$-----+++$	8	6.1946^{029}_{012}	$--+-+--++$
6	4.63714^{15}_{02}	$--+-++$	8	5.9973^{202}_{183}	$-----+-+$			
7	5.10303^{94}_{75}	$-------+$	*8	6.0100^{274}_{257}	$----++++$			

Hence, it is natural to estimate the topological entropy of the map using the following formula

$$\mathrm{h}_p(f) = \frac{\log \mathrm{P}_p}{p}. \tag{6}$$

The results are shown in Fig. 8(a). The estimate for $p = 16$ obtained using the above formula $\mathrm{h}_p(f) \approx 0.6931452$ is very close to $\log 2 \approx 0,6931472$. This is expected since all symbol sequences of length $p \leq 16$ apart from $s = (-1)$ and $s = (+1)$ are admissible, and hence $\mathrm{P}_p = 2^p - 2$ for $p \leq 16$.

The topological entropy $\mathrm{h}(\varphi)$ of the flow $\varphi(t, x)$ is defined as the topological entropy of the time–one map φ_1, i.e. $\mathrm{h}(\varphi) = \mathrm{h}(\varphi_1)$, where φ_t is defined as $\varphi_t(x) = \varphi(t, x)$. For Axiom A flows, it is known that $\mathrm{h}(\varphi) = \lim_{t\to\infty} t^{-1} \log \mathrm{P}_t$, where P_t is the number of periodic orbits with period smaller or equal to t. A faster convergence can be obtained using the 'prime number theorem' for flows [Parry & Pollicott, 1983]. It states that for Axiom A flows

$$\mathrm{P}_t \sim \frac{\exp \mathrm{h}(\varphi)t}{\mathrm{h}(\varphi)t}, \tag{7}$$

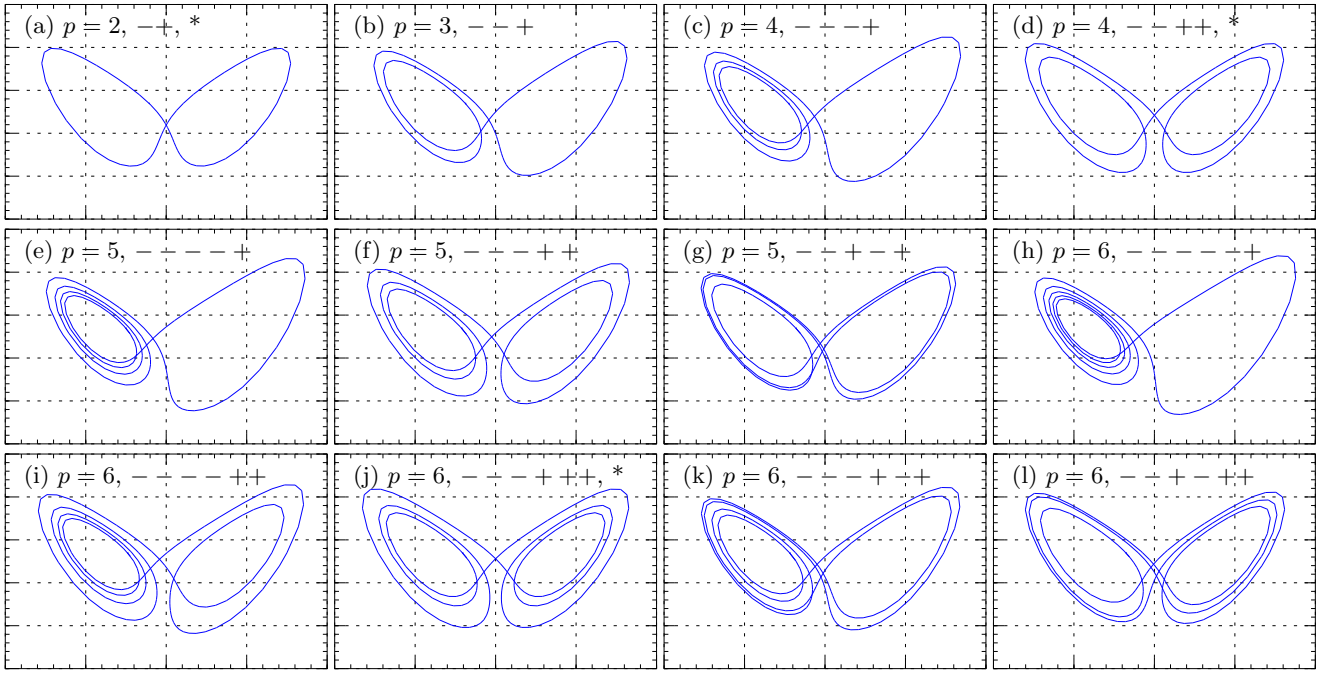

Fig. 7. The 21 shortest periodic orbits for the Lorenz system, for each pair of orbits symmetric to each other only one is plotted, the symbol '*' denotes a self-symmetric orbit

where $f(t) \sim g(t)$ means that $\frac{f(t)}{g(t)} \to 1$ as $t \to \infty$. To find the estimate h_t of the topological entropy based on P_t one solves the equation $\log \mathrm{P}_t + \log \mathrm{h}_t t - \mathrm{h}_t t = 0$. The results are plotted in Fig. 8(b). For $t > 10.0$ the approximation oscillates between 0.91 and 0.95.

3.5. *Longer periodic orbits*

This technique has also been applied to prove the existence of longer orbits with specific symbol sequences. Two examples are presented in Fig. 9.

In the first example the symbol sequence contains all possible subsequences of length $p \leq 8$. The principal period of the orbit is 486. The flow-time and the average return time belong to the intervals 369.33^{74}_{69} and 0.75995^{35}_{24}, respectively.

In the second example the symbol sequence is $s = ((-+)^{250}+)$ with the period 501. The flow-time belongs to 390.416^{52}_{42}. Hence, the average return time is in the interval 0.779274^{50}_{29} and is very close to the average return time of the shortest periodic orbit with the symbol sequence $s = (-+)$ (compare Table 3). These two orbits are very close. The distance between them (computed non-rigorously) is $2.23 \cdot 10^{-5}$. This is expected since the orbits share the symbol sequence for 500 iterations of the Poincaré map. As a consequence, the long periodic orbit is practically indistinguishable from the shortest orbit most of the time. It diverges from the shorter orbit only for a short period of time when its symbol sequence is $(\cdots++\cdots)$.

These examples show that it is possible with the method proposed to find and prove the existence of long periodic orbits with a prescribed symbol sequence. We would like to mention that some symbol sequences are easier to handle than others. Sequences containing a long subsequence of equal symbols are harder to treat. This is related to the fact that the corresponding orbits come closer to the origin, where the flow is small in magnitude. This, in turn, produces long return times, and thus the computed enclosures may suffer from huge overestimations.

4. Conclusion

We have described a symbolic dynamics based method for finding all short periodic orbits for chaotic systems. The method has been applied to the Poincaré map associated with the Lorenz system. All periodic

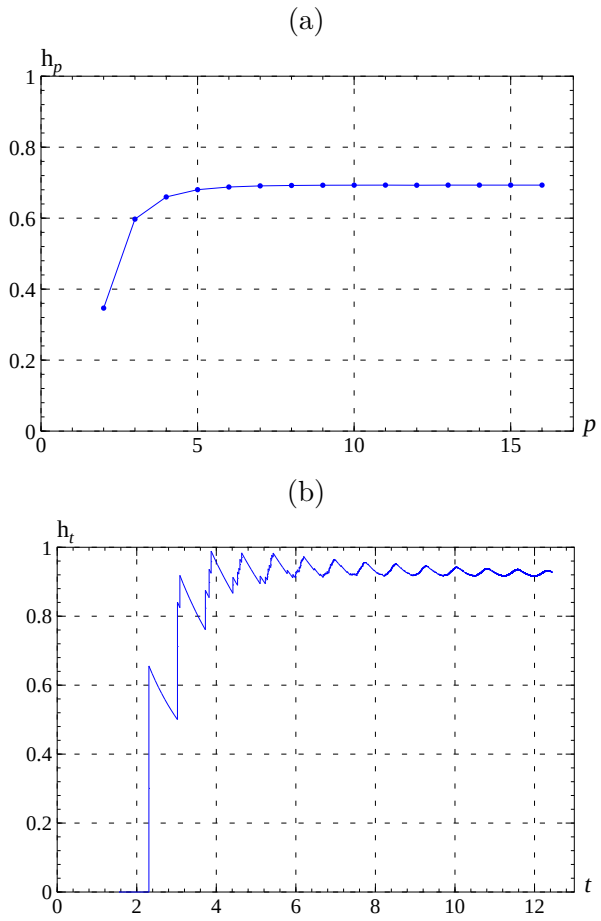

Fig. 8. Estimates for topological entropy of the map R (a) and the flow (b) based on short cycles

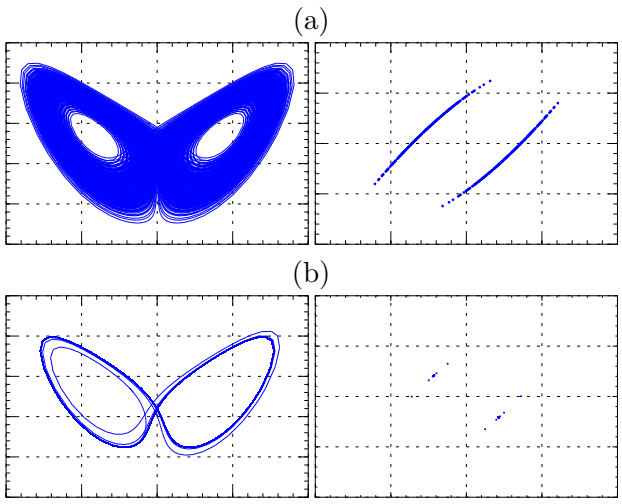

Fig. 9. Examples of long periodic orbits, (a) $p = 486$, $T \in 369.33^{74}_{69}$, (b) $p = 501$, $T \in 390.416^{52}_{42}$

orbits with the period $p \leq 16$ have been found. Several long periodic orbits with specific symbol sequences have been located and their existence have been proved.

Acknowledgments

This work was supported in part by the AGH University of Science and Technology, grant no. 11.11.120.611.

References

Benedicks, M. & Carleson, L. [1991] "The dynamics of the Hénon map," *Annals of Mathematics* **133**, 73–169.

Bielawski, S., Derozier, D. & Glorieux, P. [1994] "Controlling unstable periodic orbits by a delayed continuous feedback," *Phys. Rev. E* **49**, 971–974.

Bowen, R. [1971] "Periodic points and measures for axiom A diffeomorphisms," *Trans. Amer. Math. Soc.* **154**, 377–397.

Galias, Z. [2001] "Interval methods for rigorous investigations of periodic orbits," *Int. J. Bifurcation and Chaos* **11**, 2427–2450.

Galias, Z. [2002] "Rigorous investigations of Ikeda map by means of interval arithmetic," *Nonlinearity* **15**, 1759–1779.

Galias, Z. [2006] "Counting low-period cycles for flows," *Int. J. Bifurcation and Chaos* **16**, 2873–2886.

Galias, Z. & Zgliczyński, P. [1998] "Computer assisted proof of chaos in the Lorenz equations," *Physica D* **115**, 165–188.

Gauthier, D., Sukow, D., Concannon, H. & Socolar, J. [1994] "Stabilizing unstable periodic orbits in a fast diode resonator using continuous time-delay autosynchronization," *Phys. Rev. E* .

Krawczyk, R. [1969] "Newton-algorithmen zur bestimmung von nullstellen mit fehlerschranken," *Computing* **4**, 187–201.

Lorenz, E. [1963] "Deterministic non-periodic flow," *Journal of Atmospheric Science* **20**, 130–141.

Luzzatto, S., Melbourne, I. & Paccaut, F. [2005] "The Lorenz attractor is mixing," *Communication in Mathematical Physics* **260**, 393–401.

Mischaikow, K. & Mrozek, M. [1995] "Chaos in the Lorenz equations: a computer assisted proof," *Bull. Amer. Math. Soc.* **32**, 66–72.

Moore, R. [1966] *Interval Analysis* (Prentice Hall, Englewood Cliffs, NJ).

Neumaier, A. [1990] *Interval methods for systems of equations* (Cambridge University Press).

Ott, E., Grebogi, C. & Yorke, J. [1990] "Controlling chaos," *Phys. Rev. Lett.* **64**, 1196–1199.

Parry, W. & Pollicott, M. [1983] "An analogue of the prime number theorem for closed orbits of Axiom A flows," *Annals Math.* **118**, 573–591.

Sparrow, C. [1982] *The Lorenz equations: Bifurcations, Chaos, and Strange Attractors* (Springer Verlag, New York).

Strogatz, S. [2001] *Nonlinear Dynamics and Chaos* (Perseus Books Group).

Tucker, W. [1999] "The Lorenz attractor exists," *C. R. Acad. Sci. Paris* **328**, 1197–1202.

Tucker, W. [2002] "A rigorous ODE solver and Smale's 14th problem." *Found. Comput. Math.* **2**, 53–117.

Viswanath, D. [2003] "Symbolic dynamics and periodic orbits of the Lorenz attractor," *Nonlinearity* **16**, 1035–1056.